ISSN (Print) 1226-1750
ISSN (Online) 2233-6656
Journal of Magnetics 18(4), 417-421 (2013) http://dx.doi.org/10.4283/JMAG.2013.18.4.417

Current Density and Thickness Effects on Magnetic Properties of Electrodeposited CoPt Magnetic Films

Hyeon Soo Kim[1], Soon Young Jeong[1]*, and Su Jeong Suh[2]

[1]*Department of Physics and Research Institute of Natural Science, Gyeongsang National University, Jinju 660-701, Korea*
[2]*School of Advanced Materials Science and Engineering, Sungkyunkwan University, Suwon 440-746, Korea*

(Received 30 September 2013, Received in final form 23 October 2013, Accepted 25 October 2013)

The dominant magnetization reversal behavior of electrodeposited CoPt samples with various thicknesses deposited at different current densities was the domain wall motion by means of wall pinning. The magnetic interaction mechanism was dipolar interaction for all samples. The dipolar interaction strength was significantly affected by the sample thickness rather than by the current density, while the magnetic properties were closely related to the current density.

Keywords : CoPt magnetic film, current density, thickness, domain wall motion, wall pinning, dipolar interaction

1. Introduction

The electrodeposition method has many advantages in producing films in large quantities at comparatively low cost, with various magnetic properties, and facilitates changing the growth conditions [1-6].

The electrodeposited CoPt magnetic film with strong perpendicular magnetic anisotropy has attracted wide interest as an available material for perpendicular magnetic recording media or for the Micro Electro Mechanical System (MEMS).

In the case of magnetic recording media, the magnetic activation volume has a decisive effect on the recording density, thermal stability of recorded information, and the signal to noise ratio. The activation volume is known to be closely related to the magnetization reversal and magnetic interaction mechanism [7, 8]. In addition, these magnetic characteristics are largely affected by film deposition conditions such as current density, sample thickness, bath temperature, concentration of electrolytic solution, and the types of underlayers [9, 10]. It was found that the magnitude of the plating current density did not virtually change the composition ratio between Co and Pt in the CoPt films, but it controlled the growth rate of the films [11]. The growth rate and sample thickness are known to influence the magnetic properties because they change the grain size, surface roughness, and packing fraction [3].

In this study, we investigate the magnetization reversal mechanism and magnetic interaction behavior of CoPt films with various thicknesses grown using the electrodeposition method at different current densities. The magnetic properties are measured using a vibrating sample magnetometer (VSM) at room temperature.

2. Experiment Method

The Ta(5 nm) adhesive layer and Ru(20 nm) seed layer were grown by sputtering on the Si(1001) substrate, and the CoPt magnetic films were then galvanostatically electrodeposited onto the seed layer. A Ru seed layer was adopted to control the crystalline orientation of the CoPt structures. The electrodeposition was carried out at current densities of 10 mA/cm^2 and 20 mA/cm^2. In addition, the plating solution was maintained at a pH of 8.5 and 65°C during deposition. The samples of 10 nm, 14 nm, 18 nm, and 22 nm thicknesses were grown at 10 mA/cm^2, and the samples of 15 nm, 20 nm, and 25 nm thicknesses were grown at 20 mA/cm^2.

To investigate the behaviors of magnetization reversal and magnetic interaction, we measured the magnetic hysteresis loops in the perpendicular direction, time dependence of magnetic moment, the initial magnetization curves, minor loops, isothermal remanence (IRM), and dc demagnetization remanence (DCD) curves using a vibrating sample

*Corresponding author: Tel: +82-55-772-1404
Fax: +82-55-772-1409, e-mail: syjeong@gnu.ac.kr

magnetometer (VSM) up to a field of 10 kOe.

The time dependence of the magnetic moment was measured by first saturating the sample in the positive direction (+), then applying a reverse (–) field and monitoring the magnetic moment during 600 seconds. The positive saturating field was then reapplied and the process was repeated for an incremental interval in reverse field. In the measurement of the DCD curve, the sample was first saturated to the positive direction, and a known reverse magnetic field was then applied for 3 seconds. Subsequently, the reverse magnetic field was reduced to zero and remanent magnetization was measured. The above process was repeated with an incremented reverse field until negative saturation was reached. After demagnetizing the sample, we measured the initial magnetization curve, minor loop, and IRM curve. For the IRM curve, a constant positive field was applied to the demagnetized sample for 3 seconds and the applied field was reduced to zero, and the remanent magnetization was then measured. The above process was repeated with an incremented positive field until positive saturation was reached.

3. Results and Discussion

Figure 1 shows the coercivities (H_c) and squarenesses (M_r/M_s) for the samples deposited at 10 mA/cm^2 and 20 mA/cm^2. The values of H_c and M_r/M_s for the samples of 20 mA/cm^2 are considerably small compared to those of 10 mA/cm^2 samples. However, the thickness dependence of these quantities is nearly the same. The significant decrements of H_c and M_r/M_s for 20 mA/cm^2 samples may be due to the complex effects of changing the microstructure phases from hcp to the combined hcp and fcc phases, and decreasing the grain size and roughness [3]. Also, the thickness dependence of H_c and M_r/M_s can be

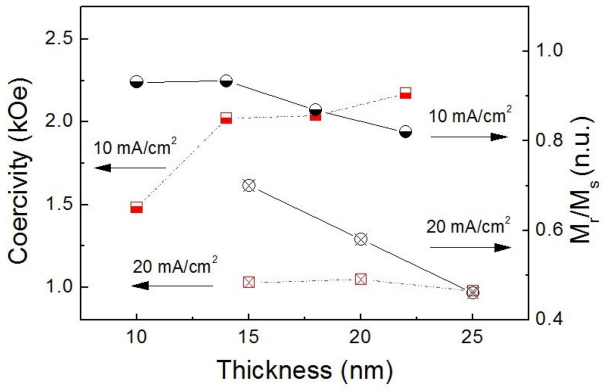

Fig. 1. (Color online) Thickness dependence of the coercivity and squareness for the samples deposited at 10 mA/cm^2 and 20 mA/cm^2.

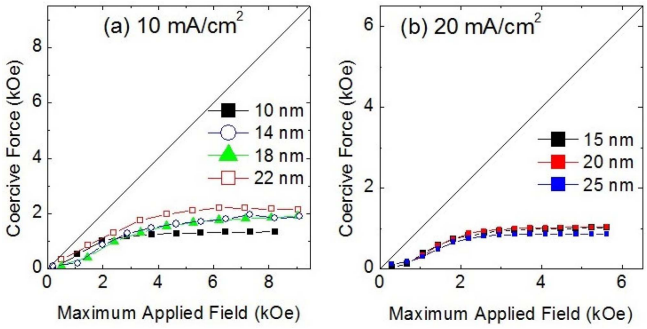

Fig. 2. (Color online) Coercive force versus maximum applied magnetic field for the samples deposited at 10 mA/cm^2 [12] and 20 mA/cm^2.

explained with the change of the crystallinity and morphology, increasing of grain size, and magnetization reversal or magnetic interaction type and its strength [3, 9]. Accordingly, it is considered that the variations of current density and sample thickness are crucial factors for determining the magnetic properties.

The magnetization reversal mechanism was identified by comparing the coercive force (H_c) with the maximum applied field (H_{max}) taken from minor loops. Fujimori *et al*. [13] suggested two different cases in which H_c is higher than H_{max}, and H_c is lower than H_{max}. According to this criterion, the former case implies nucleation, while the later implies the wall pinning or single particle rotation mechanism. The measurement results of the minor loops shown in Fig. 2 show that the coercive forces of all samples are located more at the lower region than the diagonal line because the observed H_c is smaller than H_{max}. Therefore, while it is considered that all samples make a reversal due to the domain wall motion or single particle rotation [12], the predominant reversal mechanism remains unclear.

The initial magnetization curves shown in Fig. 3 indicate that the initial curve is more declined to the magnetic field axis as the thickness is increased. Such phenomenon can be interpreted as a typical wall pinning.

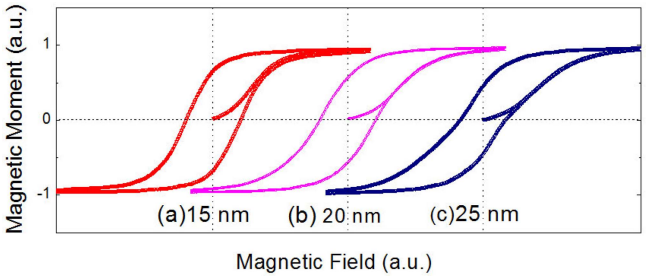

Fig. 3. (Color online) Initial magnetization curves for different thicknesses for the samples deposited at 20 mA/cm^2.

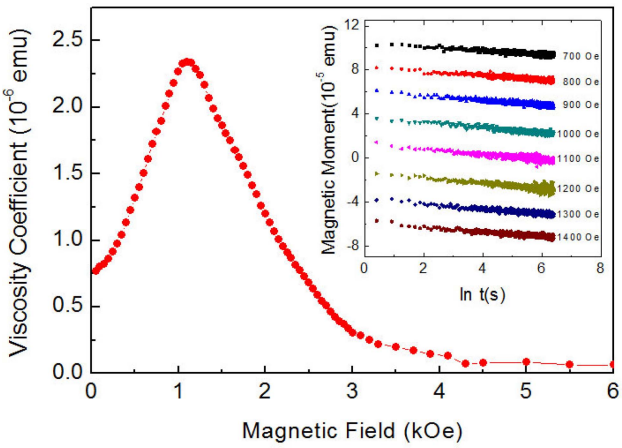

Fig. 4. (Color online) Magnetic field dependence of the magnetic viscosity coefficient for the 15 nm thick samples deposited at 20 mA/cm^2. Inner box indicates the magnetic moment decay curves.

From the measurement results of the minor loops and the initial curves, it may be reasonable to assert that all samples make a reversal through domain wall motion.

The time dependence of the magnetic moment is known as a qualitative method used to understand the magnetization reversal behavior. The moment decay curve shows quite different behavior, depending on the distribution of energy barrier due to thermal activation. If the energy barrier distribution is appropriately changed, the change in magnetization satisfies the following relation, $M(H, t) = M_o(H, t_o) \pm S(t)\ln t$. Here, M and M_o are the net magnetizations of time t and t_o, respectively, and S is the magnetic viscosity coefficient which is generally positioned near the coercivity. If the time dependence of the magnetic moment complies with this relationship, the wall pinning is regarded as the main magnetization reversal behavior for the samples [14].

Figure 4 shows the field dependence of the magnetic moment decay curves and magnetic viscosity coefficient for the 15 nm sample. As shown in this figure, the decay curves are clearly linear with ln$t$ over a measuring time span. The measured moment decay curves of all the other samples also show the typical wall pinning feature as for the 15 nm sample. From the analyzed results of minor loops, initial curves, and time dependence of magnetic moment, it is assumed that the magnetization reversal of all samples is made from the domain wall motion controlled by the pinning of the domain wall.

To investigate the dominant reversal phenomenon in more detail, the magnetic field dependence of irreversible magnetic susceptibilities ($\chi_{irr}^{irm}(H)$, $\chi_{irr}^{dcd}(H)$) was examined by employing the IRM and DCD curves. The IRM differential $\chi_{irr}^{irm}(H)$ reflects the energy barrier distribution of the pinning sites, while the DCD differential $\chi_{irr}^{dcd}(H)$ represents the energy barrier distribution of the nucleation from the occurred saturated state. Therefore, the information on the dominant reversal mechanism can be obtained from the relative position of the maximum irreversible magnetic susceptibility.

As shown in Fig. 5, the position of the peak $\chi_{irr}^{dcd}(H)$ falls to the left-hand side of the position of peak $\chi_{irr}^{irm}(H)$; i.e., the nucleation field (H_N) is located at the lower magnetic field region compared to the wall pinning field (H_P). Furthermore, as the thickness of the samples increases, the pinning field also increases, but the nucleation field decreases. The samples deposited at 10 mA/cm^2 and 20 mA/cm^2 show the same thickness dependency as shown in Fig. 6. However, the field difference between H_N and H_P is increased with increasing sample thickness for all samples. Such phenomena result in the pinning of the domain walls and a reduction in hysteresis loop squareness as mentioned above. Consequently, it is concluded that the reversal mechanism for the 10 mA/cm^2 and 20 mA/cm^2 samples is the domain wall motion controlled by the wall pinning and the role of the wall pinning becomes more apparent as the current density and sample thickness are increased.

The magnetic interaction mechanism and its strength

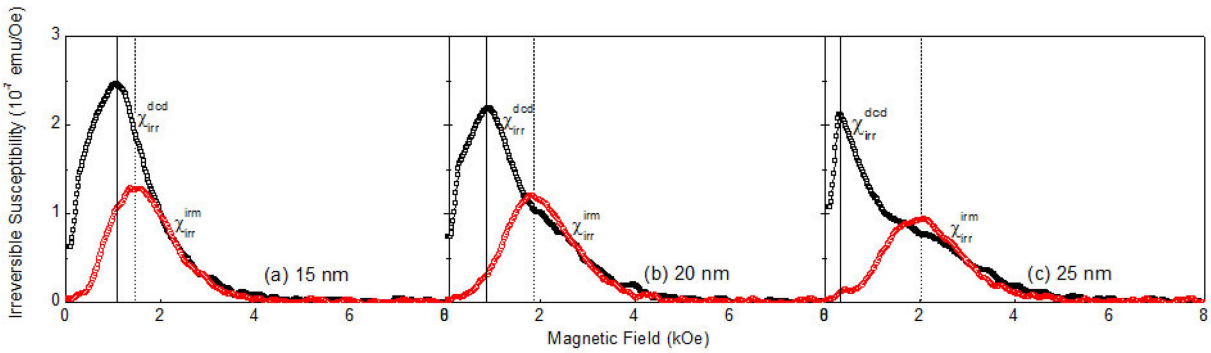

Fig. 5. (Color online) Irreversible susceptibilities obtained from the DCD and IRM curves for the samples deposited at 20 mA/cm^2.

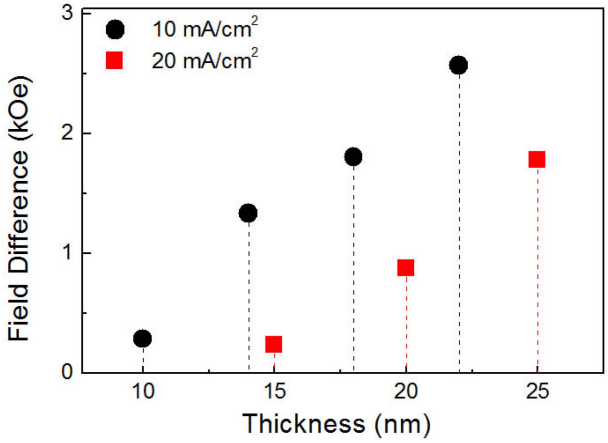

Fig. 6. (Color online) Thickness dependence of the magnetic field difference for the samples deposited at 10 mA/cm^2 and 20 mA/cm^2. Magnetic field difference is defined as the field gap between the position of the nucleation field and the pinning field.

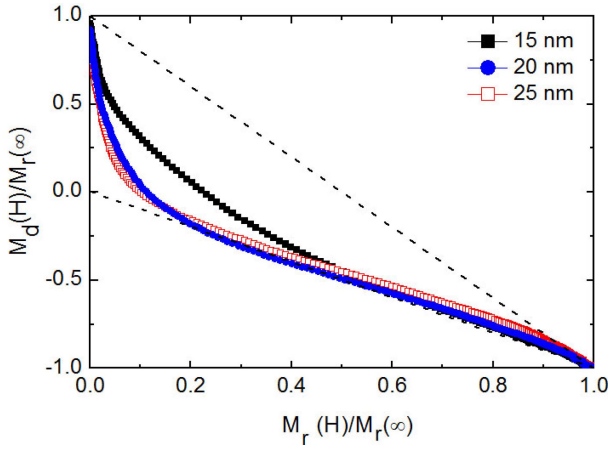

Fig. 7. (Color online) Henkel plots obtained from the DCD and IRM remanence curves for the samples of different thicknesses deposited at 20 mA/cm^2.

can be determined by adopting the interaction field factor, Henkel plot, and Wohlfarth equation. The interaction field factor $IFF = (H_{cd} - H_{ci})/H_c$ was defined by Corradi and Wohlfarth [15]. Here, H_{ci}, H_{cd}, and H_c are obtained from the IRM, DCD, and the magnetic hysteresis curves, respectively. As the measured values of H_{ci} are larger than H_{cd} for all samples, the calculated *IFF* values are –0.33, –0.67, –1.03, and –1.08 for the 12 nm, 16 nm, 18 nm and 22 nm thick samples, respectively. In addition, all of the samples deposited at 20 mA/cm^2 also show negative *IFF* values. The negative *IFF* values indicate that the nature of magnetic interaction is the dipolar interaction and its strength is increased as the sample thickness is increased.

The Henkel plot has been extensively used to investigate the magnetic interaction for the recording media as well as the permanent magnets. In the case of a magnetic system composed of non-interacting single domain particles, the dependence of the two remanence curves on the interactions between the grains follows the Wolhfarth formula [16] $m_d(H) = 1–2m_r(H)$. Here, $m_d(H) = m_d(H)/M_r(\infty)$, $m_r(H) = m_r(H)/M_r(\infty)$, and H constitute the magnetic field applied in the reversed direction. The Wohlfarth formula was first introduced by Henkel [17] to describe the effect of interactions between grains. Figure 7 shows the Henkel plots obtained from the IRM and DCD curves for the samples deposited at 20 mA/cm^2. It appeared that the plots are not linear but rather meet the criterion of $m_d(H) < 1–2m_r(H)$. This criterion suggests that the intergrain interactions promote the demagnetization. Therefore, the main magnetic interaction is the dipolar interaction, as shown in the 10 mA/cm^2 samples [12]. According to I. Zana *et al.* [18], the non-magnetic phases P (or P compounds) were precipitated at the grain boundaries while electrodepositing. Therefore, the dipolar interaction in our samples may be resulted in these non-magnetic phases.

The type of magnetic interaction and its strength can also be examined by using the modified Wohlfarth relation [19] expressed in $\delta M(H) = m_d(H)–[1–2m_r(H)]$. As mentioned above, the negative $\delta M(H)$ refers to the dipolar interaction, while the positive $\delta M(H)$ refers to the exchange interaction. The modified Wohlfarth relation thus describes the interaction type, while the area of the $\delta M(H)$ curve, which is defined as $|\delta M(H)area| = \int_0^{H_a} \delta M(H)dH$, may be a good measure of the interaction strength.

Figure 8 shows the $\delta M(H)$ curves of the 20 mA/cm^2 samples with different thicknesses. As the applied magnetic field increases, $\delta M(H)$ decreases, reaches a peak, and then converges to zero. The $\delta M(H)$ variation implies that the interactions between the grains may be closely related to

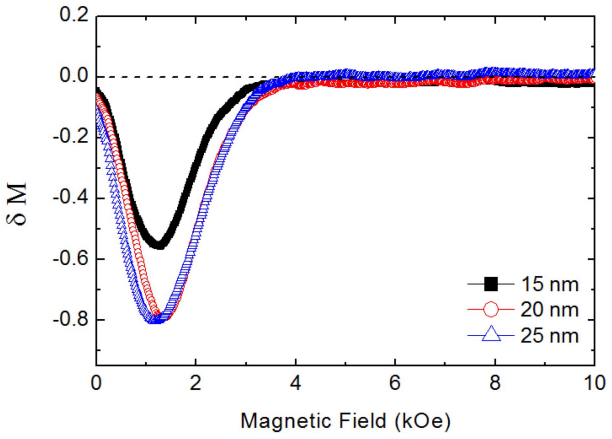

Fig. 8. (Color online) Applied field dependence of $\delta M(H)$ for the samples of different thicknesses deposited at 20 mA/cm^2.

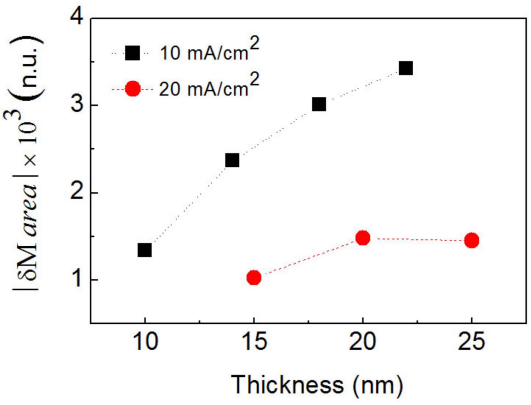

Fig. 9. (Color online) Thickness dependence of $|\delta M(H)area|$ for the samples deposited at 10 mA/cm^2 and 20 mA/cm^2.

the magnetization state of the samples.

The strength of the magnetic interaction can be estimated by applying the area of the $\delta M(H)$ curves. The estimated $|\delta M(H)area|$ for the samples with various thicknesses is grown at different current densities and is represented in Fig. 9. As shown in this figure, the $|\delta M(H)area|$ for the samples of 10 mA/cm^2 is much larger than that of the samples prepared at 20 mA/cm^2. In addition, the $|\delta M(H)area|$ is increased with increasing thickness. The thickness dependence of the $\delta M(H)$ peak values and area are appropriately matched with the change of field position in the maximum viscosity coefficients and the decrease of *IFF* values. Thus, the significant increase of the $\delta M(H)$ peak and $|\delta M(H)area|$ with increasing thickness reveals that the thickness is an important factor to control the interaction strength in the CoPt samples.

In conclusion, the dipolar interaction is the predominant interaction mechanism, and while its strength is slightly related to the current density, it is remarkably influenced by the sample thickness in our samples. The observed increase in dipolar interaction with increasing thickness can be ascribed to the growth of grains size as well as the intricate shapes of grains. The variations of $\delta M(H)$ means that the interaction between grains may be largely related to the magnetization state of the samples.

4. Conclusion

The CoPt samples with various thicknesses deposited at different plating current densities exhibited a domain wall motion by means of wall pinning. In addition, the enhancement of wall pinning is more pronounced as the sample thickness is increased. This enhancement is well explained by broadening the magnetic field difference between the field position of peak $\chi_{irr}^{dcd}(H)$ and peak $\chi_{irr}^{dcd}(H)$, and decreasing of the maximum viscosity coefficients.

The magnetic interaction mechanism was a dipolar interaction for all samples. The interaction strength was more significantly affected by the sample thickness than by the current density, while the perpendicular magnetic characteristics were closely related to the current density which controlled the growing rate of samples.

Acknowledgements

This work was supported by the research funds of the 2012 Gyeongsang National University Professor Sabbatical Year Program and part of the work was supported by a research fund from the physics department of GNU in 2012.

References

[1] N. V. Myung, D. Y. Park, M. Schwartz, K. Nobe, H. Yang, C.-K. Yang, and J. W. Judy, Proc. Electrochem. Soc. **PV2000-29** (2000).
[2] I. Zana, G. Zangari, J.-W. Park, and M. G. Allen, J. Magn. Magn. Mater. **272**, e1775 (2004).
[3] I. Zana, G. Zangari, and M. Shamsuzzoha, J. Magn. Magn. Mater. **292**, 266 (2005).
[4] M. Ghidini, G. Asti, C. Pernechele, L. Prejbeanu, M. Solzi, and G. Zangari, J. Magn. Magn. Mater. **316**, e112 (2007).
[5] G. Bottoni, D. Candolfo, and A. Cecchetti, J. Appl. Phys. **81**, 3809 (1997).
[6] H. Ohmori and A. Maesaka, J. Appl. Phys. **91**, 8635 (2002).
[7] M. P. Sharrock, IEEE Trans. Magn. **26**, 193 (1990).
[8] P. Lu and S. H. Charap, J. Appl. Phys. **75**, 5768 (1994).
[9] M. Ghidini, A. Lodi-Rizzini, C. Pernechele, M. Solzi, R. Pellicelli, G. Zangari, and P. Vavassori, J. Magn. Magn. Mater. **322**, 1576 (2010).
[10] Fernando, M. F. Rhen, and J. M. D. Coeys, J. Magn. Magn. Mater. **272**, e883 (2004).
[11] I. Zana and G. Zangari, J. Magn. Magn. Mater. **272**, 1698 (2004).
[12] S. H. Kim, J. D. Lee, S. Y. Jeong, H. C. Lee, and S. J. Suh, J. Kor. Mag. Soc. **21**, 151 (2011).
[13] H. Fujimori, O. Suzuki N. Hosoya, X. B. Yang, and H. Morita, IEEE Trans. **30**, 4038 (1994).
[14] T. Thomson and K. O'Grady, J. Appl. Phys. **30**, 1566 (1997).
[15] A. R. Corradi and E. P. Wohlfarth, IEEE Trans. Magn. **14**, 861 (1978).
[16] E. P. Wohlfarth, J. Appl. Phys. **29**, 595 (1958).
[17] O. Henkel, Phys. Status Solid. **7**, 919 (1964).
[18] I. Zana, G. Zangari, and M. Shamsuzzoha, J. Electrochem. Soc. **151**, C637 (2004).
[19] P. E. Kelly, K. O'Grady, P. I. Mayo, and R. W. Chantrell, IEEE Trans. Magn. **25**, 3881 (1989).